A Stochastic Economic Growth Model with Health Capital and State-Dependent Probabilities

Davide La Torre [*] Simone Marsiglio[†] Franklin Mendivil[‡]
Fabio Privileggi[§]

Forthcoming in Chaos, Solitons & Fractals

Abstract

We analyze a simple stochastic model of economic growth in which physical and health capital accumulation jointly contribute to determine long run economic growth. Health capital is subject to random shocks via the effects of behavioral changes: unpredictable changes in individuals' attitude toward healthy behaviors may reduce the effectiveness of health services provision; this in turn, by reducing the production of new health capital, lowers economic production activities negatively affecting economic growth. Unlike the extant literature, we assume that the probability with which such random shocks occur is not constant but state-dependent. Specifically, the probability that behavioral changes will negatively impact on health capital and economic growth depends on the level of economic development, proxied by the relative abundance of health capital with respect to physical capital. We show that our model's dynamics can be converted into an iterated function system with state-dependent probabilities which converges to an invariant self-similar measure supported on a (possibly fractal) compact attractor. We develop a numerical method to approximate the invariant distribution to illustrate its features in specific model's parametrizations, exemplifying thus the effects of state-dependent probabilities on the model's steady state.

Keywords: Health Capital; Iterated Function Systems; State-Dependent Probabilities; Foias Operator
JEL Classification: C61, C63, O40

1 Introduction

The importance of random shocks for economic outcomes and macroeconomic dynamics is well known since the seminal work by [7]. A large body of studies analyze from different points of

[*]SKEMA Business School, Sophia Antipolis, France and Department of Economics, Management, and Quantitative Methods, University of Milan, Italy. Email: davide.latorre@unimi.it.

[†]University of Pisa, Department of Economics and Management, via Cosimo Ridolfi 10, 56124 Pisa, Italy. Email: simone.marsiglio@unipi.it.

[‡]Department of Mathematics and Statistics, Acadia University, Wolfville, Canada. Email: franklin.mendivil@acadiau.ca.

[§]Department of Economics and Statistics "Cognetti de Martiis", University of Turin, Torino, Italy. Email: fabio.privileggi@unito.it.

view the implications of uncertainty on economic growth (see [26] for a survey). Several of these papers analyze the random dynamics associated with economic growth models showing that they can eventually converge to invariant measures supported on fractal sets [23]. The fractal nature of the steady state of such stochastic growth models has been extensively analyzed lately, both in purely dynamic setting ([17], [27]) and in frameworks with agents' optimization ([19], [20], [21], [22]), showing that the support of the invariant measure can take the form of different fractal sets, including the Cantor set ([23], [19], [20], [21], [22] and [13]), the Sierpinski gasket ([12], [13]) or the Barnsley's fern ([15],[16]). To the best of our knowledge, all these works rely upon the assumption that the probability with which shocks occur is constant over time. Even if this setting is useful to characterize macroeconomic dynamics in a simple and intuitive way, it precludes us from analyzing the implications of important phenomena, and in particular how the stage of economic development affects the probability with which shocks may occur. Several studies argue that developing countries are more vulnerable to shocks than industrialized economies [32], and thus that the entire process of economic development may be characterized by path-dependency ([10], [25], [18]): after a certain level of development is achieved, further development is more likely to occur. Understanding thus the implications of path-dependency for economic development and macroeconomic outcomes is crucial to develop a realistic theory of economic growth. This paper wishes to make a first contribution in this direction by proposing a simple stochastic growth model in which probabilities are state-dependent. State-dependent probabilities are a straightforward generalization of constant probabilities which allow to explain the path-dependency phenomenon and to enrich the set of possible outcomes for the model, shedding some light on the mutual links between economic shocks and economic development.

Specifically, we analyze a simple two-sector stochastic purely dynamic model of economic growth in which physical and health capital accumulation jointly contribute to determine long run economic growth ([33], [1], [4]). Health capital measures the health status of the population which can be improved through the purposive provision of health services. Health capital determines the level of productivity of the labor force and thus it represents an important input in economic production activities. Both the final consumption good and health services are produced by combining physical and health capital, but the production of health services is subject to random shocks via the effects of behavioral changes: unpredictable changes in individuals' attitude toward healthy behaviors may reduce the effectiveness of the health services provided; this in turn, by reducing the production of new health capital, lowers economic production activities negatively affecting economic growth in the long run. The probability with which these shocks occur endogenously depends on the economy's level of development measured by the relative abundance of health capital with respect to physical capital, meaning that according to its specific development stage an economy may be more or less likely to face a negative shock with detrimental effects on long run economic growth. We show that this model can be converted into a contractive iterated function system (IFS) with state-dependent probabilities (SDP) which, under rather general conditions, converges to an invariant self-similar measure supported on a (possibly fractal) compact attractor. Iterated function systems with state-dependent probabilities (IFSSDP) have received much attention in the mathematics literature, mostly in the context of state-dependent Markov processes with invariant measures ([3], [29], [14]), but to the best of our knowledge they have never been discussed in economics. In this paper we develop a novel application of IFSSDPs in macroeconomic theory to shed some light on the effects of state-dependent probabilities on the economic dynamics and the steady state of a stochastic growth model.

The paper proceeds as follows. Section 2 reviews some well-known concepts on the IFS theory and it focuses in particular on the theory of IFSSDP. Section 3 introduces our stochastic growth

model with state-dependent probabilities and, after a brief discussion on the dynamical features of its deterministic counterpart, shows how its random dynamics can be converted into an affine IFSSDP. Section 4 presents a numerical method to approximate the invariant measure of affine IFSSDPs, which is then applied in Section 5 to illustrate, for a given parameterization of the growth model, how the characteristics of the invariant measure associated to our IFSSDP are affected by different choices of the state-dependent probability generating it. Section 6 as usual presents concluding remarks and highlights directions for future research.

2 Iterated Function Systems

In this section we review some basic concepts and results in the theory of iterated function systems. We first discuss the case in which probabilities are constant, and since this case is well-known we will try to be as brief as possible (similar but more detailed discussions can be found in [13], [16]). We then move to the less-known case in which probabilities are state dependent, and we will discuss with more depth the implications of such state-dependency.

2.1 Constant Probabilities

Let (X, d) be a compact metric space. An N-map *Iterated Function System* (IFS) on X, $\mathbf{w} = \{w_1, \ldots, w_N\}$, is a set of N contraction mappings on X, *i.e.*, $w_i : X \to X$, $i = 1, \ldots, N$, with contraction factors $c_i \in [0, 1)$ (see [2], [8], [11]). Associated with an N-map IFS, one can construct the following set-valued mapping $\hat{\mathbf{w}}$ on the space $\mathcal{H}(X)$ of nonempty compact subsets of X:

$$\hat{\mathbf{w}}(S) := \bigcup_{i=1}^{N} w_i(S), \qquad S \in \mathcal{H}(X).$$

The distance between sets can be measured by means of the Hausdorff distance h defined on $\mathcal{H}(X)$ as follows:

$$h(A, B) = \max\left\{\sup_{x\in A}\inf_{y\in B} d(x, y), \sup_{x\in B}\inf_{y\in A} d(x, y)\right\}.$$

The pair $(\mathcal{H}(X), h)$ is a compact (and then complete) metric space.

Theorem 1 ([8])**.** *For $A, B \in \mathcal{H}(X)$,*

$$h(\hat{\mathbf{w}}(A), \hat{\mathbf{w}}(B)) \leq cH(A, B) \qquad \textit{where } c = \max_{1\leq i\leq N} c_i < 1.$$

The following result states the contractivity of the operator $\hat{\mathbf{w}}$ with respect to the Hausdorff distance.

Corollary 1. *There exists a unique set $\bar{A} \in \mathcal{H}(X)$ such that*

$$\bar{A} = \hat{\mathbf{w}}(\bar{A}) = \bigcup_{i=1}^{N} w_i(\bar{A}).$$

Moreover, for any $B \in \mathcal{H}(X)$, $h\left(\bar{A}, \hat{\mathbf{w}}^t B\right) \to 0$ as $t \to \infty$.

The set $\bar{A} \in \mathcal{H}(X)$ is called the *attractor* of the IFS $\mathbf{w}$ as it satisfies the properties which define an attractor of a general dynamical system.[1]

An N-map *iterated function system with (constant) probabilities* $(\mathbf{w}, \mathbf{p})$ is an N-map IFS $\mathbf{w}$ with associated probabilities $\mathbf{p} = \{p_1, \ldots, p_N\}$, $\sum_{i=1}^{N} p_i = 1$.

Let $\mathcal{M}(X)$ denote the set of probability measures on (Borel subsets of) X and d_{MK} the Monge-Kantorovich distance on this space. For $\mu, \nu \in \mathcal{M}(X)$ the Monge-Kantorovich metric is defined as

$$d_{MK}(\mu, \nu) = \sup_{f \in Lip_1(X)} \left[\int f \, d\mu - \int f \, d\nu \right],$$

where $Lip_1(X) = \{f : X \to \mathbb{R} : |f(x) - f(y)| \leq d(x, y)\}$. The metric space $(\mathcal{M}(X), d_{MK})$ is compact (and then complete) [2], [8]. If X is not compact but only complete then a first-moment condition needs to be imposed to guarantee the completeness of $(\mathcal{M}(X), d_{MK})$.

Associated with an N-map IFSP is a mapping $M : \mathcal{M} \to \mathcal{M}$, often referred to as the *Foias operator*, defined as follows. Let $\nu = M\mu$ for any $\mu \in \mathcal{M}(X)$. Then for any measurable set $S \subset X$,

$$\nu(S) = (M\mu)(S) = \sum_{i=1}^{N} p_i \, \mu\left(w_i^{-1}(S)\right).$$

Theorem 2 ([8]). *For $\mu, \nu \in \mathcal{M}(X)$,*

$$d_{MK}(M\mu, M\nu) \leq c \, d_{MK}(\mu, \nu).$$

Corollary 2. *There exists a unique measure $\bar{\mu} \in \mathcal{M}(X)$, the* invariant measure *of the IFSP $(\mathbf{w}, \mathbf{p})$, such that*

$$\bar{\mu}(S) = (M\bar{\mu})(S) = \sum_{i=1}^{N} p_i \bar{\mu}\left(w_i^{-1}(S)\right). \tag{1}$$

Moreover, for any $\nu \in \mathcal{M}(X)$, $d_{MK}(\bar{\mu}, M^t\nu) \to 0$ as $t \to \infty$.

Theorem 3 ([8]). *The support of the invariant measure $\bar{\mu}$ of an N-map IFSP $(\mathbf{w}, \mathbf{p})$ is the attractor $\bar{A}$ of the IFS $\mathbf{w}' = \{w_i : p_i > 0\}$, i.e.,*

$$supp\, \bar{\mu} = \bar{A}.$$

Example 1. *The following two-map IFS on $X = [0, 1]$,*

$$w_1(x) = \frac{1}{2}x, \qquad w_2(x) = \frac{1}{2}x + \frac{1}{2},$$

has attractor $A = [0, 1]$. Let $p_1 \equiv p_2 \equiv 1/2$. It is well known that the invariant measure $\bar{\mu}$ of this IFSP is the (uniform) Lebesgue measure on $[0, 1]$. This is simple to see by verifying (1) for $S = [a, b] \subseteq [0, 1]$.

[1] We recall that a dynamical system is a pair (X, ϕ) where (X, d) is a metric space and $\phi : X \to X$ is a continuous map. A set $A \subset X$ is said to be a global attractor for (X, ϕ) if: i) $\phi(A) \subseteq A$, ii) $\lim_{n \to +\infty} d'(A, \phi^n(x_0)) = 0$ for any $x_0 \in X$, where d' is the distance point-to-set and $\phi^n(x_0) = \phi(\phi(...(\phi(x_0))))$ is the n^{th} iterate of ϕ applied to x_0 (or the orbit generated by x_0). Of course if $A = \{\bar{x}\}$ is a singleton, then $\bar{x}$ is a fixed point of ϕ. Banach fixed point theorem guarantees the existence of a unique fixed point that is also a global attractor under completeness of X and contractivity of ϕ with respect to d.

Note that, while in this paper we assume that all the maps w_i in the IFS are contractive, the contractivity of M only requires *average contractivity*, $\sum_i p_i c_i < 1$ [30].

2.2 State-Dependent Probabilities

We now consider the case in which the probabilities, $p_i, 1 \leq i \leq N$, associated with an N-map IFS $\mathbf{w}$ are state-dependent, *i.e.*, $p_i : X \to [0,1]$ such that

$$\sum_{i=1}^{N} p_i(x) = 1, \qquad \text{for all } x \in X. \tag{2}$$

In the literature a lot of attention has been devoted to IFSs with state-dependent probabilities in particular in the context of state-dependent Markov processes with invariant measures [29].

The result is an N-map *IFS with state-dependent probabilities* (IFSSDP).

Example 2 (Affine probability functions)**.** *In the special case $X = [0,1] \subset \mathbb{R}$ with affine probabilities $p_i(x) = \xi_i x + \eta_i$, substitution into (2) along with the fact that the functions x and 1 are linearly independent over [0,1] yields the following conditions on the ξ_i and η_i,*

$$\sum_{i=1}^{N} \xi_i = 0\,, \qquad \sum_{i=1}^{N} \eta_i = 1.$$

Only two other conditions must be imposed, namely, (i) $0 \leq p_i(0) \leq 1$ and $0 \leq p_i(1) \leq 1$ for $1 \leq i \leq N$, which lead to the following additional constraints,

$$0 \leq \eta_i \leq 1, \qquad 0 \leq \xi_i + \eta_i \leq 1, \qquad 1 \leq i \leq N.$$

These constraints also imply that $-1 \leq \xi_i \leq 1$. In the special case $\xi_i = 0$, $1 \leq i \leq N$, the IFSSDP reduces to an IFSP with constant probabilities $p_i = \eta_i$, $1 \leq i \leq N$.

Associated with an N-map IFSSDP, $(\mathbf{w}, \mathbf{p})$, there is a Foias operator $M : \mathcal{M}(X) \to \mathcal{M}(X)$, defined as follows. Let $\nu = M\mu$ for any $\mu \in \mathcal{M}(X)$. Then for any measurable set $S \subset X$,

$$\nu(S) = M\mu(S) = \sum_{i=1}^{N} \int_{w_i^{-1}(S)} p_i(x)\, d\mu(x)\,. \tag{3}$$

Theorem 4 ([14])**.** *Given M as defined in (3), then M maps $\mathcal{M}(X)$ to itself. In other words, if $\mu \in \mathcal{M}(X)$, then $\nu = M\mu \in \mathcal{M}(X)$.*

Under appropriate conditions, the above Foias operator can be contractive with respect to the Monge-Kantorovich metric.

Theorem 5 ([14])**.** *Let (X,d) be a compact metric space and $(\mathbf{w}, \mathbf{p})$ an N-map IFSSDP with IFS maps $w_i : X \to X$ with contraction factors $c_i \in [0,1)$. Furthermore, assume that the probabilities $p_i : X \to \mathbb{R}$ are Lipschitz functions, with Lipschitz constants $K_i \geq 0$. Let $M : \mathcal{M}(X) \to \mathcal{M}(X)$ be the Foias operator associated with this IFSSDP, as defined in (3). Then for any $\mu, \nu \in \mathcal{M}(X)$,*

$$d_{MK}(M\mu, M\nu) \leq (c + KDN)\, d_{MK}(\mu, \nu)\,,$$

where $c = \max_i c_i$, $K = \max_i K_i$ *and* $D = diam(X) < \infty$. *If* $c + KDN < 1$ *then there exists a unique measure* $\bar{\mu} \in \mathcal{M}(X)$, *the* invariant measure *of the IFSSDP, such that* $M\bar{\mu} = \bar{\mu}$. *Moreover, for any* $\nu \in \mathcal{M}(X)$, $d_{MK}(\bar{\mu}, M^t\nu) \to 0$ *as* $t \to \infty$.

However, the operator M needs not to be contractive with respect to the Monge-Kantorovich metric in order to have a fixed point. In fact, by the Schauder fixed point theorem, as long as all the $p_i(x)$s are continuous there is at least one invariant measure for M. The following examples exhibit more than one invariant measure.

Example 3. *We return to the two-map IFS on* $X = [0,1]$ *of Example 1,*

$$w_1(x) = \frac{1}{2}x, \qquad w_2(x) = \frac{1}{2}x + \frac{1}{2},$$

and consider two state dependent probabilities $p_1(x) = 1 - x$ *and* $p_2(x) = x$. *In this case the two Dirac measures* δ_0 *and* δ_1, *concentrated at the points* 0 *and* 1 *respectively, are both fixed points and thus it is not possible for the Foias operator to be contractive. Moreover, for any* $\xi \in [0,1]$, *the measure* $\mu = \xi\delta_0 + (1-\xi)\delta_1$ *is a fixed point of the Foias operator.*

We now describe the so-called *Chaos Game* for an IFS with probabilities. Start with $x_0 \in X$, and define the sequence $x_t \in X$ by

$$x_{t+1} = w_{\sigma_t}(x_t),$$

where $\sigma_t \in \{1, 2, \ldots, N\}$ is chosen according to the probabilities $p_i(x_t)$ (that is, $P[\sigma_t = i] = p_i(x_t)$). We note that the sequence (x_t) is a Markov chain with values in X.

The following theorem (from results in [3], [9]) gives conditions as to when the IFSSDP has a unique stationary distribution $\bar{\mu}$ and the Chaos Game "converges" to $\bar{\mu}$ in a distributional sense.

Theorem 6 ([3], [9])**.** *Suppose that there is a* $\delta > 0$ *so that* $p_i(x) \geq \delta$ *for all* $x \in X$ *and* $i = 1, 2, \ldots, N$ *and suppose further that the moduli of continuity of the* p_i*s satisfy Dini's condition (see [3], [9]). Then there is a unique stationary distribution* $\bar{\mu}$ *for the Foias operator. Furthermore, for each continuous function* $f : X \to \mathbb{R}$,

$$\frac{1}{t+1}\sum_{h=0}^{t} f(x_h) \to \int_X f(x)\ d\bar{\mu}(x).$$

where the sequence $\{x_h\}_{h=0}^t$ *is generated by the Chaos Game described above, that is* $x_{h+1} = w_{\sigma_h}(x_h)$, *and* $\sigma_h \in \{1, 2, \ldots, N\}$ *is chosen according to* $P[\sigma_h = i] = p_i(x_h)$.

Theorem 6 can be used to show the following result.

Corollary 3. *Suppose that the IFSSDP* $\{\mathbf{w}, p_i\}$ *satisfies the hypothesis of Theorem 6. Then the support of the invariant measure* $\bar{\mu}$ *of the* N*-map IFSSDP* $(\mathbf{w}, \mathbf{p})$ *is the attractor* $\bar{A}$ *of the IFS* $\mathbf{w}$, *i.e.,*

$$supp\,\bar{\mu} = \bar{A}.$$

Notice that the support of the invariant measure of an IFSPDP depends only on the family of IFS maps $\mathbf{w}$ and not on the family of probabilities p_i.

Example 4. *Modifying Example 3 slightly by using*

$$p_1(x) = 1 - \beta - (1 - 2\beta)x, \quad \text{and} \quad p_2(x) = (1 - 2\beta)x + \beta,$$

for $0 < \beta < 1$, we obtain an IFSSDP which satisfies the conditions of Theorem 6 and thus has a unique invariant measure. Notice that the probability functions from Example 3 correspond to the case $\beta = 0$.

Notice that if p_i are not continuous then the IFSSDP might have more than one invariant measure (in fact, continuity is not enough – see [29]).

The following theorem allows us to characterize the singularity of the self-similar measure associated to an IFS with state-dependent probability in the case of two linear maps having the same slope. The proof follows by noticing that whenever the common slope λ satisfies $\lambda < 1/2$ the invariant measure $\bar{\mu}_\lambda$ is supported on a Cantor set with zero Lebesgue measure.

Proposition 1. *Take the two-map IFS $\{\lambda x, \lambda x + (1-\lambda)\}$ on $X = [0,1]$ where $\lambda \in (0,1)$ along with the two probability functions $p_1(x) = p(x)$ and $p_2(x) = 1 - p(x)$ on $[0,1]$. Assume that $\inf\{p(x) : 0 \leq x \leq 1\} > 0$ and that and that p is Hölder continuous. Let $\bar{\mu}_\lambda$ be the invariant measure of this state-dependent IFS. If $0 \leq \lambda < 1/2$ then $\bar{\mu}_\lambda$ is singular with respect to the Lebesgue measure.*

3 The Model

We propose a discrete time stochastic growth model driven by physical and health capital accumulation: while physical capital is a rival good, health capital is a nonrival good. Our novel contribution consists of allowing the probabilities with which shocks occur to be state-dependent. As our main goal is to analyze the effects of such state-dependent probabilities on the dynamics of the economic system, for the sake of simplicity we completely abstract from agents' optimization and we focus on a purely dynamic Solow-type [28] setting. As in [31], the unique final consumption good, y_t, is produced through a constant returns to scale Cobb-Douglas production function employing health capital, h_t, and a certain share of physical capital, k_t, as follows: $y_t = \theta (uk_t)^\alpha h_t^{1-\alpha}$, where $\theta > 0$ is a fixed productivity parameter, $0 < \alpha < 1$ is the physical capital share of GDP and $0 < u < 1$ an exogenously given share of physical capital allocated to final good production. Physical capital is accumulated through investment activities, to which an exogenous share of output is devoted: $k_{t+1} = sy_t$, where $0 < s < 1$ is the saving rate. Health capital accumulates thanks to the provision of health services, g_t, as follows: $h_{t+1} = g_t$. Health services are produced through a Cobb-Douglas production function employing the existing level of health capital and the share of physical capital not used in the production of the final good. This represents a situation in which the provision of health services is relatively intensive in physical capital, meaning that in order to achieve further improvements in the health status of the population it is important to invest in physical infrastructure (hospitals, machines, medical equipment). However, such production activities are also subject to multiplicative random shocks, z_t, so that the total production of health services is $g_t = z_t [(1-u) k_t]^\beta h_t^{1-\beta}$, where $0 < \beta < 1$ is the elasticity of health services production with respect to physical capital, and z_t is a random component measuring the effect of behavioral changes which may reduce the effectiveness of activities aimed to improve the overall health status in the population resulting in increases in the health capital. Indeed, the diffusion of antivax sentiments, the spread of risky sexual behavior and the growing reliance on junk food are all examples of how changes in individuals' health attitude can affect the effectiveness of health services potentially harming the entire economy. For the sake of simplicity, we abstract from physical and health capital depreciation without loss of generality.

3.1 The Deterministic Dynamics

As the dynamics characterizing our model present a sufficiently rich scenario already in the deterministic version, we deem it worth spend in a few words on this setting before analyzing how random shocks may affect such dynamics. By assuming that $z_t \equiv z$ is constant through time (*i.e.*, non random), with $0 < z \leq 1$, the model's dynamics are determined by the following system of difference equations:

$$\begin{cases} k_{t+1} = s\theta \left(uk_t\right)^{\alpha} h_t^{1-\alpha} \\ h_{t+1} = z \left[\left(1-u\right) k_t\right]^{\beta} h_t^{1-\beta} \\ k_0 \text{ and } h_0 > 0 \text{ given.} \end{cases} \tag{4}$$

According to the specific model's parametrization, three scenarios are possible and the system (4) may exhibit:

1. convergence to a unique non trivial steady state whenever parameters z, s, θ, u and α satisfy a certain condition; such a steady state, however, depends on the initial conditions k_0 and h_0;

2. sustained growth of both k_t and h_t if the saving rate s is larger than the threshold value characterizing the previous scenario;

3. asymptotic extinction of the economy, *i.e.*, $k_t \to 0^+$ and $h_t \to 0^+$ as $t \to \infty$, if the saving rate s is smaller than the threshold value characterizing the first scenario.

Specifically, any steady state for system (4) must satisfy:

$$\begin{cases} k = s\theta u^{\alpha} \left(k\right)^{\alpha} \left(h\right)^{1-\alpha} \\ h = z \left(1-u\right)^{\beta} \left(k\right)^{\beta} \left(h\right)^{1-\beta} \end{cases} \iff \begin{cases} \left(\dfrac{h}{k}\right)^{1-\alpha} = \dfrac{1}{s\theta u^{\alpha}} \\ \left(\dfrac{h}{k}\right)^{\beta} = z \left(1-u\right)^{\beta} \end{cases} \iff \begin{cases} \dfrac{h}{k} = \dfrac{1}{\left(s\theta u^{\alpha}\right)^{\frac{1}{1-\alpha}}} \\ \dfrac{h}{k} = z^{\frac{1}{\beta}} \left(1-u\right). \end{cases} \tag{5}$$

The last system of equations can be satisfied only if

$$\left(s\theta u^{\alpha}\right)^{-\frac{1}{1-\alpha}} = z^{\frac{1}{\beta}} \left(1-u\right),$$

that is, only if the saving rate satisfies:

$$\bar{s} = \frac{1}{\theta u^{\alpha} \left[z^{\frac{1}{\beta}} \left(1-u\right)\right]^{1-\alpha}}. \tag{6}$$

Note that, as $0 < u < 1$ and $0 < \bar{s} < 1$ must hold, the following condition must be met:

$$\theta > \frac{1}{u^{\alpha} \left[z^{\frac{1}{\beta}} \left(1-u\right)\right]^{1-\alpha}}, \tag{7}$$

which, as $0 < z \leq 1$ and $0 < u < 1$, implies necessarily that $\theta > 1$.

It is immediately seen from system (5) that the steady state is naturally defined in terms of the ratio h/k; hence, it is convenient to explicitly introduce the new variable health to physical capital ratio:

$$\chi_t = \frac{h_t}{k_t}. \tag{8}$$

Therefore, a *steady state* is any pair (h, k) satisfying

$$\chi^* = \frac{h}{k} \equiv z^{\frac{1}{\beta}} (1-u)\,; \tag{9}$$

this represents a situation of balanced development in which the input ratio (*i.e.*, the health to physical capital ratio) is constant. This steady state is globally stable and the economy naturally tends to converge to such a long run situation of balanced development. Whenever the physical capital ratio is different than the constant $1-u$, then it will change over time. Specifically, when $h_t/k_t > 1-u$ there is an excessive level of health capital with respect to physical capital and the former decreases while the latter increases as time elapses; the opposite occurs when $h_t/k_t < 1-u$. This represents a situation of unbalanced development in which the input ratio keeps changing over time. The effects of unbalances on economic growth have been analyzed by several studies ([24], [5], [6]), and our model as we shall clarify later suggests that such unbalances may occur endogenously through the realization of shocks. To see how the transition towards the steady state works let us compute the growth rates of k_t and h_t:

$$\begin{aligned}\bar{\gamma}_t^k = \frac{k_{t+1}-k_t}{k_t} &= \frac{\bar{s}\theta u^\alpha k_t^\alpha h_t^{1-\alpha}}{k_t} - 1 = \frac{\theta u^\alpha}{\theta u^\alpha \left[z^{\frac{1}{\beta}}(1-u)\right]^{1-\alpha}} \left(\frac{h_t}{k_t}\right)^{1-\alpha} - 1 \\ &= \left[\frac{\chi_t}{z^{\frac{1}{\beta}}(1-u)}\right]^{1-\alpha} - 1 \end{aligned} \tag{10}$$

$$\bar{\gamma}_t^h = \frac{h_{t+1}-h_t}{h_t} = \frac{z(1-u)^\beta k_t^\beta h_t^{1-\beta}}{h_t} - 1 = z(1-u)^\beta \left(\frac{k_t}{h_t}\right)^\beta - 1 = \left[\frac{z^{\frac{1}{\beta}}(1-u)}{\chi_t}\right]^\beta - 1, \tag{11}$$

where in the second equality of the first line we used (6). From the expressions above it is immediately seen that whenever $\chi_t > z^{\frac{1}{\beta}}(1-u)$ the physical capital exhibits a positive growth rate and, at the same time, the health capital exhibits a negative growth rate, while the signs of the growth rates are the opposite if $\chi_t < z^{\frac{1}{\beta}}(1-u)$; this establishes that the steady state is globally stable.[2]

Finally, having in mind the introduction of random shocks to our dynamical system in the next Subsection, it is interesting to study the dynamics (4) for values of the saving rate different than that defined in (6). Using (8), system (4) can be reduced to a one-dimensional dynamic in the variable χ_t:

$$\chi_{t+1} = \frac{h_{t+1}}{k_{t+1}} = \frac{z(1-u)^\beta k_t^\beta h_t^{1-\beta}}{s\theta u^\alpha k_t^\alpha h_t^{1-\alpha}} = \frac{z(1-u)^\beta}{s\theta u^\alpha}\left(\frac{h_t}{k_t}\right)^\lambda = z\Lambda\chi_t^\lambda \tag{12}$$

[2]There is, however, a caveat: as the steady state $\chi^* = h/k \equiv z^{\frac{1}{\beta}}(1-u)$ in (9) is defined by the ratio between health and physical capital, any pair (h, k) having ratio $z^{\frac{1}{\beta}}(1-u)$ defines a steady state, possibly corresponding to values of h and k very far apart. By the (opposite) monotonicity of the transition dynamics of k_t and h_t defined by their growth rates in (10) and (11), we deduce that each different steady state χ^* depends on the initial conditions, (k_0, h_0). In other words, only economies starting with high levels of both physical and health capital converge to steady states envisaging high stationary values of physical and health capital. We may thus claim that the deterministic version of our model under the assumption that the saving rate satisfies (6) exhibits indeterminacy in the sense that there exist a continuum of stable steady states, each dependent on the initial condition (k_0, h_0).

where

$$\Lambda = \frac{(1-u)^{\beta}}{s\theta u^{\alpha}} \qquad \text{and} \qquad \lambda = \alpha - \beta.$$

In the following we shall assume that $\alpha > \beta > 0$ so to always have $0 < \lambda < 1$, which, in turn, implies that the one-dimensional dynamic defined by (12) has a unique globally stable steady state defined by:

$$\chi^{*} = (z\Lambda)^{\frac{1}{1-\lambda}} = \left[\frac{z\,(1-u)^{\beta}}{s\theta u^{\alpha}}\right]^{\frac{1}{1-\lambda}} = \left[\frac{z\,(1-u)^{\beta}}{s\theta u^{\alpha}}\right]^{\frac{1}{1-\alpha+\beta}}. \tag{13}$$

The growth rates of k_t and h_t along the steady state χ^{*} defined in (13) turn out to be the same:

$$\begin{aligned}
\gamma_t^k &= \frac{k_{t+1}-k_t}{k_t} = s\theta u^{\alpha}\left(\frac{h_t}{k_t}\right)^{1-\alpha} - 1 = s\theta u^{\alpha}\left(\chi^{*}\right)^{1-\alpha} - 1 = s\theta u^{\alpha}\left[\frac{z\,(1-u)^{\beta}}{s\theta u^{\alpha}}\right]^{\frac{1-\alpha}{1-\alpha+\beta}} - 1 \\
&= (s\theta u^{\alpha})^{\frac{\beta}{1-\alpha+\beta}}\left[z\,(1-u)^{\beta}\right]^{\frac{1-\alpha}{1-\alpha+\beta}} - 1 \qquad (14) \\
\gamma_t^h &= \frac{h_{t+1}^{*}-h_t^{*}}{h_t^{*}} = z\,(1-u)^{\beta}\left(\frac{k_t}{h_t}\right)^{\beta} - 1 = z\,(1-u)^{\beta}\left(\frac{1}{\chi^{*}}\right)^{\beta} - 1 \\
&= z\,(1-u)^{\beta}\left[\frac{s\theta u^{\alpha}}{z\,(1-u)^{\beta}}\right]^{\frac{\beta}{1-\alpha+\beta}} - 1 \\
&= (s\theta u^{\alpha})^{\frac{\beta}{1-\alpha+\beta}}\left[z\,(1-u)^{\beta}\right]^{\frac{1-\alpha}{1-\alpha+\beta}} - 1, \qquad (15)
\end{aligned}$$

which is consistent with the property of balanced development in steady state in which both variables k_t and h_t grow at the same rate over time. Specifically, if $s > \bar{s}$ we have:

$$\begin{aligned}
s > \bar{s} = \frac{1}{\theta u^{\alpha}\left[z^{\frac{1}{\beta}}\,(1-u)\right]^{1-\alpha}} \quad &\Longleftrightarrow \quad s\theta u^{\alpha}\left[z^{\frac{1}{\beta}}\,(1-u)\right]^{1-\alpha} > 1 \\
\Longleftrightarrow \quad (s\theta u^{\alpha})^{\frac{\beta}{1-\alpha+\beta}}\left[z^{\frac{1}{\beta}}\,(1-u)\right]^{\frac{\beta(1-\alpha)}{1-\alpha+\beta}} > 1 \quad &\Longleftrightarrow \quad (s\theta u^{\alpha})^{\frac{\beta}{1-\alpha+\beta}}\left[z\,(1-u)^{\beta}\right]^{\frac{1-\alpha}{1-\alpha+\beta}} > 1,
\end{aligned}$$

which implies that both growth rates of k_t and h_t in (14) and (15) are positive, that is, when $s > \bar{s}$ system (4) describes an economy that asymptotically converges to a balanced growth path in which both health and physical capital grow at the same positive constant rate. Conversely, if $s < \bar{s}$ both growth rates of k_t and h_t in (14) and (15) are negative and the economy asymptotically converges to a balanced growth path that lead to extinction as $t \to \infty$.

3.2 Adding Random Shocks to Health Capital Production

We now assume that coefficient z is a random variable affecting health capital production, so that the stochastic model's dynamics can be summarized by the following system of difference equations:

$$\begin{cases} k_{t+1} = s\,(uk_t)^{\alpha}\,h_t^{1-\alpha} \\ h_{t+1} = z_t\,[(1-u)\,k_t]^{\beta}\,h_t^{1-\beta} \\ k_0, h_0 > 0 \text{ and } z_0 \in \{r, 1\} \text{ given.} \end{cases}$$

The random shock $\{z_t\}_{t=0}^{\infty}$ is a Bernoulli process taking values $0 < r < 1$ and 1 with probabilities $p(h_t/k_t) = p(\chi_t)$ and $1 - p(h_t/k_t) = 1 - p(\chi_t)$, respectively. Therefore, at each time t, z_t can take only two values with state-dependent probabilities; specifically, the fact that probabilities depend on the health to physical capital ratio implies that the realization of shocks is related to the past evolution of both types of capital, implying a path-dependency in the macroeconomic dynamics. In particular, what matters in determining the probability of shocks is the relative abundance of the two forms of capital which is a proxy for the level of economic development. As mentioned earlier, economic development is balanced if the physical to health capital ratio remains constant over time, while it is unbalanced when the ratio changes over time. The fact that the probability of shocks depends on the physical to health capital ratio implies that unbalanced development is the result of the realizations of random shocks. By recalling that random shocks represent the effects of behavioral changes, our model suggests that the effectiveness of public activities aimed to improve the overall health status in the economy changes with the level of development. For example, more developed economies may be conducive to the diffusion of junk foods with detrimental effects on health capital accumulation (i.e., $p' < 0$), or conducive of safer sexual behavior with beneficial effects on health capital accumulation (i.e., $p' > 0$). It is not so clear which of these cases is more realistic to consider, thus in the following we will not impose a priori any restriction on the relation between $p(\cdot)$ and economic development, but we will analyze how the results will change when $p' \gtreqless 0$.

The one-dimensional dynamic of the reduced model expressed by the health to physical capital ratio variable $\chi_t = h_t/k_t$, to which the probability $p(\chi_t)$ actually depends, is the same as in (12), only with the random shock z_t replacing the constant z:

$$\chi_{t+1} = z_t \Lambda \chi_t^{\lambda} \tag{16}$$

with $\Lambda = (1-u)^{\beta} / (s\theta u^{\alpha})$ and $\lambda = \alpha - \beta$, satisfying $\alpha > \beta > 0$ so to always have $0 < \lambda < 1$. The one-dimensional dynamics described by (16) is straightforward: it has an attractive set to which the system is eventually being trapped defined as the interval

$$[\chi_r^*, \chi_1^*] = \left[(r\Lambda)^{\frac{1}{1-\lambda}}, \Lambda^{\frac{1}{1-\lambda}}\right] = \left[\left(\frac{r(1-u)^{\beta}}{s\theta u^{\alpha}}\right)^{\frac{1}{1-\alpha+\beta}}, \left(\frac{(1-u)^{\beta}}{s\theta u^{\alpha}}\right)^{\frac{1}{1-\alpha+\beta}}\right],$$

whose endpoints are the globally stable steady state of the model defined in (13) for $z = r$ and $z = 1$ respectively. As $t \to \infty$ the variable χ_t jumps from one feasible value to another in the interval $[\chi_r^*, \chi_1^*]$ according to a stochastic process governed by the state-dependent probabilities $p(\chi_t)$ and $1 - p(\chi_t)$ that, as it will be shown in the sequel, eventually converges to an invariant measure whose support may be the whole interval $[\chi_r^*, \chi_1^*]$ or some (fractal) subset of it.

However, recasting the original dynamics followed by the pair (k_t, h_t) is not simple: from the previous discussion on the deterministic model counterpart we know that the pattern followed by such dynamics depends on the relative value of the saving rate s with respect to the values of parameters θ, u, α and on the realization of the random shock $z_t \in \{r, 1\}$ [see condition (6)]. Specifically, assuming that condition

$$\theta > \frac{1}{u^{\alpha}\left[r^{\frac{1}{\beta}}(1-u)\right]^{1-\alpha}} \tag{17}$$

holds—which implies that condition (7) hold as well for $z = 1$—and defining

$$\bar{s}_1 = \frac{1}{\theta u^{\alpha} (1-u)^{1-\alpha}}, \qquad \bar{s}_r = \frac{1}{\theta u^{\alpha} \left[r^{\frac{1}{\beta}} (1-u) \right]^{1-\alpha}}, \tag{18}$$

whenever $0 < p(\chi_t) < 1$ three scenarios may occur.

1. If $\bar{s}_1 \leq s \leq \bar{s}_r$, when the time t shock realization is $z_t = 1$ the system finds itself on a transition trajectory that, if $z_t = 1$ were to hold forever, would eventually approach a balanced growth path characterized by sustained growth (or to some steady state defined by $\chi_1^* = h/k \equiv 1 - u$ if $s = \bar{s}_1$). However, as $0 < p(\chi_t) < 1$, at some future date $\tau_1 > t$ the realization $z_{\tau_1} = r$ must occur with probability 1; at such date the system jumps on a different type of transition trajectory that, if $z_t = r$ were to hold forever, would eventually converge to balanced growth path leading to extinction (or to some steady state defined by $\chi_r^* = h/k \equiv r^{\frac{1}{\beta}} (1-u)$ if $s = \bar{s}_r$). The economy, however, cannot vanish entirely (or converge to the smaller steady state $\chi_r^* = r^{\frac{1}{\beta}} (1-u)$ if $s = \bar{s}_r$) as there is another future date $\tau_2 > \tau_1$ at which $z_{\tau_2} = 1$ again and the system reverses back to a new transition trajectory pushing toward sustained growth (or toward the larger steady state $\chi_1^* = 1 - u$ if $s = \bar{s}_1$). Because all jumps from one regime to the other—sustained growth vs. decay—happen from ever changing values of (k_t, h_t), depending on how many times the shock value z_t remained constant before, the system actually wanders around in an unpredictable way.

2. If $s > \bar{s}_r$ the system exhibits features that, at least qualitatively, are easier to classify, as in this case the economy converges to paths characterized by sustained balanced growth. The system actually jumps from transition trajectories converging to sustained balanced growth at different constant rates depending on the shock realization z_t, with a smaller constant growth rate associated to the $z_t = r$ realization and a larger constant growth rate associated to the $z_t = 1$ realization.

3. Similarly, if $s < \bar{s}_1$ the economy converges to balanced paths characterized by constant decay implying that the economy vanishes asymptotically regardless of the realization of the Bernoulli process of shocks $\{z_t\}_{t=0}^{\infty}$. The latter process realization establishes a path characterized by jumps between transition trajectories converging to balanced paths defined by different rates of decay, the faster associated to the occurrence of $z_t = r$ realizations and the slower associated to the occurrence of $z_t = 1$ realizations.

3.3 The associated log-linearized dynamics

Let us focus on the simpler one-dimensional random dynamical system defined by (16):

$$\chi_{t+1} = z_t \Lambda \chi_t^{\lambda},$$

$$\text{where } \Lambda = (1-u)^{\beta} / (s\theta u^{\alpha}) \text{ and } \lambda = \alpha - \beta, \text{ with } \alpha > \beta > 0 \text{ so that } 0 < \lambda < 1.$$

Through an appropriate log-transformation it is possible to recast (16) into a topologically equivalent one. Specifically, defining the new variable:

$$x_t = -\frac{1-\lambda}{\ln r} \ln \chi_t + 1 + \frac{\ln \Lambda}{\ln r}, \tag{19}$$

the new random dynamic system becomes:

$$x_{t+1} = \lambda x_t + (1-\lambda)\left(1 - \frac{\ln z_t}{\ln r}\right),$$

which can be rewritten as follows:

$$\begin{cases} x_{t+1} = \lambda x_t & \text{with probability } \tilde{p}(x_t) \\ x_{t+1} = \lambda x_t + (1-\lambda) & \text{with probability } 1 - \tilde{p}(x_t), \end{cases} \tag{20}$$

where

$$\tilde{p}(x_t) \equiv p(\chi_t) = p\left(\frac{h_t}{k_t}\right) = p\left[(r\Lambda)^{\frac{1}{1-\lambda}}\left(r^{-\frac{1}{1-\lambda}}\right)^{x_t}\right], \tag{21}$$

which follows from (19) since

$$\begin{aligned} \ln \chi_t &= \frac{\ln r + \ln \Lambda}{1-\lambda} - \frac{\ln r}{1-\lambda} x_t = \frac{\ln(r\Lambda)}{1-\lambda} - \frac{\ln r}{1-\lambda} x_t = \ln\left[(r\Lambda)^{\frac{1}{1-\lambda}}\right] + \ln\left[\left(r^{-\frac{1}{1-\lambda}}\right)^{x_t}\right] \\ &= \ln\left[(r\Lambda)^{\frac{1}{1-\lambda}}\left(r^{-\frac{1}{1-\lambda}}\right)^{x_t}\right], \end{aligned}$$

which, in turn, implies that

$$\chi_t = (r\Lambda)^{\frac{1}{1-\lambda}}\left(r^{-\frac{1}{1-\lambda}}\right)^{x_t}.$$

From the results in Section 2.2 we know that the IFSSDP (20) defined on the space $X = [0,1]$ converges to a unique invariant measure $\bar{\mu}_\lambda$ supported on the attractor $\bar{A}$ defined in Corollary 1 whenever $\inf\{\tilde{p}(x) : 0 \leq x \leq 1\} > 0$ and $\tilde{p}$ is Hölder continuous. Moreover, according to Proposition 1, if $\lambda < 1/2$ the attractor $\bar{A}$ is a Cantor-like set and the invariant measure $\bar{\mu}_\lambda$ is singular with respect to the Lebesgue measure.

In the rest of the paper we will focus on the IFSSDP given by (20), in which the maps are linear. In the next section we develop a numerical method to approximate its invariant measure and show the implications of state-dependent probabilities on the fractal steady state of our stochastic growth model.

4 A Method to Approximate the Invariant Measure

In this section we focus on the affine IFSSDP $\{w_1(x), w_2(x), p(x)\}$ defined by

$$\begin{cases} w_1(x) = \lambda x & \text{with prob. } p(x) \\ w_2(x) = \lambda x + (1-\lambda) & \text{with prob. } 1 - p(x) \end{cases} \tag{22}$$

on $X = [0,1]$ where $\lambda \in (0, 1/2]$ and $p : [0,1] \to (0,1)$ is a Hölder continuous function representing the state-dependent probability $p(x_{t-1})$ of moving from $x_{t-1} \in [0,1]$ to $x_t = w_1(x_{t-1}) = \lambda x_{t-1}$ after the t^{th} iteration of the IFSSDP, while $1 - p : [0,1] \to (0,1)$ represents the state-dependent probability $1 - p(x_{t-1})$ of moving from $x_{t-1} \in [0,1]$ to $x_t = w_2(x_{t-1}) = \lambda x_{t-1} + (1-\lambda)$ after the t^{th} iteration of the IFSSDP. In other words, the function $p(x)$ denotes the probability of reaching the lowest of the two maps in (22), $w_1(x)$, after one period when in $t-1$ the system is on x, while $1 - p(x)$ denotes the probability of reaching the highest of the two maps in (22), $w_2(x)$, after one period when in $t-1$ the system is on x. The assumption that $0 < \lambda \leq 1/2$ implies that the IFSSDP is (almost) non overlapping, *i.e.*, whenever $\lambda < 1/2$ the images of the maps w_1, w_2 do not

overlap and the attractor of the system is a Cantor-like set, that we will denote by λ-Cantor set, while when $\lambda = 1/2$ the images of the maps w_1, w_2 overlap only on the (zero Lebesgue measure) point $1/2$ and the attractor of the system is the full interval $[0,1]$.

Our aim is to provide an iterative algorithm capable of approximating the unique invariant measure $\bar{\mu}_\lambda$ supported on the attractor of the IFSSDP (22). To this purpose we exploit the very intuitive process defined by the Chaos game according to the random dynamics described by (22). Let $\mathcal{B}[0,1]$ be the σ-algebra of Borel measurable subsets of $[0,1]$ and $\mathcal{P}[0,1]$ the space of probability measures on $\mathcal{B}[0,1]$. Recall the following definitions of the Hutchinson and Foias operators respectively, $W : [0,1] \to [0,1]$ and $M : \mathcal{P}[0,1] \to \mathcal{P}[0,1]$:

$$W(A) = w_1(A) \cup w_2(A), \qquad \text{for all } A \subseteq [0,1], \tag{23}$$

$$M\mu(B) = \int_{w_1^{-1}(B)} p(x)\, d\mu(x) + \int_{w_2^{-1}(B)} [1 - p(x)]\, d\mu(x), \qquad \text{for all } B \in \mathcal{B}[0,1] \tag{24}$$

where $w_\sigma(A)$ denotes the image of the set A through w_σ and $w_\sigma^{-1}(B)$ denotes the set $\{x \in [0,1] : w_\sigma(x) \in B\}$, $\sigma = 1, 2$.

The algorithm starts from the uniform density on $[0,1]$, $\mu_0(x) \equiv 1$ for a.e. $x \in [0,1]$, and then applies iteratively the Foias operator in (24) to generate the t^{th} marginal distribution of the system supported over the t^{th} pre-fractal generated by the Hutchinson operator in (23). To keep the algorithm simple and efficient we approximate each iteration of M, $\mu_t(\cdot) = M\mu_{t-1}(\cdot)$, by measuring the mass produced by M on each component (sub-interval) of the t^{th} pre-fractal and originating from the masses supported over each component of the pre-fractals generated by the same iteration of W applied on the $(t-1)^{th}$ pre-fractal. Specifically, we first generate all components of the pre-fractal after the t^{th} iteration of W starting from $A_0 = [0,1]$ and then we put a uniformly distributed mass on each component according to $M\mu_{t-1}$, where μ_{t-1} is the set of rectangular masses on the components of the pre-fractal obtained after the $(t-1)^{th}$ iteration of M, starting with the rectangle $[0,1]^2$ representing the uniform distribution $\mu_0(x) \equiv 1$ over $A_0 = [0,1]$. Indeed, the algorithm is based on the following two core procedures.

1. The following recursion produces the t^{th} pre-fractal as union of the images of the maps w_1, w_2 evaluated on the $(t-1)^{th}$ pre-fractal according to

$$\begin{aligned}
A_0 &= [0,1] \\
A_1 &= w_1(A_0) \cup w_2(A_0) = w_1([0,1]) \cup w_2([0,1]) = [0,\lambda] \cup [1-\lambda, 1] \\
A_2 &= w_1(A_1) \cup w_2(A_1) = w_1([0,\lambda] \cup [1-\lambda,1]) \cup w_2([0,\lambda] \cup [1-\lambda,1]) \\
&= \left[0, \lambda^2\right] \cup \left[\lambda - \lambda^2, \lambda\right] \cup \left[1-\lambda, 1-\lambda+\lambda^2\right] \cup \left[1-\lambda^2, 1\right] \\
&\vdots \\
A_t &= w_1(A_{t-1}) \cup w_2(A_{t-1}) \\
&= \left[0, \lambda^t\right] \cup \left[\lambda^{t-1} - \lambda^t, \lambda^{t-1}\right] \cup \cdots \cup \left[1-\lambda^{t-1}, 1-\lambda^{t-1}+\lambda^t\right] \cup \left[1-\lambda^t, 1\right].
\end{aligned} \tag{25}$$

   Each pre-fractal A_t is made up of 2^t components (sub-intervals), each of size (Lebesgue measure) λ^t; such components are disjoint (they do not overlap) whenever $\lambda < 1/2$, in which case $\lim_{t\to\infty} A_t$ is the λ-Cantor set. Each component is thus an interval that we will denote by $[x_{t,i}, x_{t,i+1}]$ of length $x_{t,i+1} - x_{t,i} = \lambda^t$, for $i = 1, 3, 5, \ldots, 2^{t+1} - 1$. The key step in each iteration is the split of each component of the $(t-1)^{th}$ pre-fractal with length λ^{t-1}, $[x_{t-1,i}, x_{t-1,i+1}]$ into two smaller components of length λ^t in the t^{th} pre-fractal, corresponding

to its two distinct images through the maps w_1 and w_2. As we keep track of all components in each pre-fractal by their endpoints, $x_{t,i}, x_{t,i+1}$, the idea is to exploit the recursion (25) so as to let the procedure generate four endpoints, $x_{t,j}$, $x_{t,j+i}$, $x_{t,j+2}$, $x_{t,j+3}$, corresponding to two components of the t^{th} pre-fractal, out of the originating unique preimage $[x_{t-1,i}, x_{t-1,i+1}]$ through one of the maps w_σ, for $\sigma = 1, 2$, which is one single component of the $(t-1)^{th}$ pre-fractal. In other words, we generate the two new components in the t^{th} pre-fractal as the intervals $[x_{t,j}, x_{t,j+i}] = [x_{t-1,i}, x_{t-1,i} + \lambda^t]$ and $[x_{t,j+2}, x_{t,j+3}] = [x_{t-1,i+1} - \lambda^t, x_{t-1,i+1}]$, which is nothing else than the standard procedure to generate the λ-Cantor set: to remove the middle interval from each component in the $(t-1)^{th}$ pre-fractal. Note that, besides the counter t, in this first part two indexes are needed: i and j, the former increasing by 2 after each split of the $(t-1)^{th}$ component into the two t^{th} components (the next left endpoint of the $(t-1)^{th}$ component is $i+3$) and the latter increasing by 4 (the next first left endpoint of the third component born after the t^{th} iteration is $j+5$).

2. While the generation of all components $[x_{t,i}, x_{t,i+1}]$ in the t^{th} pre-fractal is pursued sequentially according to recursion (25), the building of the marginal probabilities ('rectangular masses') supported on them is obtained by computing the two masses originating from the same $(t-1)^{th}$ rectangular mass supported on one single $(t-1)^{th}$ component as they are being transformed into new masses over the two intervals corresponding to the images of each map w_1 and w_2. Thus, such newly born pairs of masses are put on intervals which are far apart: one in the first half of $[0,1]$, to which $\mathrm{Im}(w_1)$ belongs, and the other in the second half of $[0,1]$, to which $\mathrm{Im}(w_2)$ belongs. Specifically, the rectangle denoting the mass supported on each component $[x_{t-1,i}, x_{t-1,i+1}]$ of the $(t-1)^{th}$ pre-fractal is being split into two masses, each supported on the two distinct components of the t^{th} pre-fractal corresponding to the image sets $w_1([x_{t-1,i}, x_{t-1,i+1}])$ and $w_2([x_{t-1,i}, x_{t-1,i+1}])$, according to the weights defined by the fixed state-dependent probabilities $p(y)$ and $1-p(y)$ respectively,[3] both with $y \in [x_{t-1,i}, x_{t-1,i+1}]$. Let us denote by $\mu_{t-1,i}$ the (constant) mass supported on the component $[x_{t-1,i}, x_{t-1,i+1}]$—that is, the area of the rectangle with base $[x_{t-1,i}, x_{t-1,i+1}]$—in the $(t-1)^{th}$ pre-fractal. Hence, in principle the Foias operator in (24) would define the two masses $\mu_{t,i}$ and $\mu_{t,2^{t-1}+i}$, supported respectively on the components $w_1([x_{t-1,i}, x_{t-1,i+1}])$ and $w_2([x_{t-1,i}, x_{t-1,i+1}])$ of the t^{th} pre-fractal, as[4]

$$\mu_{t,i} = \int_{x_{t-1,i}}^{x_{t-1,i+1}} p(y)\,\mu_{t-1,i}dy = \mu_{t-1,i}\int_{x_{t-1,i}}^{x_{t-1,i+1}} p(y)\,dy$$
$$\mu_{t,2^{t-1}+i} = \int_{x_{t-1,i}}^{x_{t-1,i+1}} [1-p(y)]\,\mu_{t-1,i}dy = \mu_{t-1,i}\int_{x_{t-1,i}}^{x_{t-1,i+1}} [1-p(y)]\,dy.$$

That is, as is apparent from the right hand sides above, $\mu_{t,i}$ and $\mu_{t,2^{t-1}+i}$ are originated by the same (constant) mass $\mu_{t-1,i}$, but are weighted according to the integrals $\int_{x_{t-1,i}}^{x_{t-1,i+1}} p(y)\,dy$ and $\int_{x_{t-1,i}}^{x_{t-1,i+1}} [1-p(y)]\,dy$ respectively. However, as the interval of integration, $[x_{t-1,i}, x_{t-1,i+1}]$, has length $\lambda^{t-1} < 1$ and the state-dependent probabilities $p(y)$ and $1-p(y)$ sum up to 1 for any $y \in [x_{t-1,i}, x_{t-1,i+1}]$, the two integral values $\int_{x_{t-1,i}}^{x_{t-1,i+1}} p(y)\,dy$ and $\int_{x_{t-1,i}}^{x_{t-1,i+1}} [1-p(y)]\,dy$

[3]From now on we will denote by y the argument of the place-dependent probabilities to avoid confusion with the endpoints $x_{t-1,i}$ and $x_{t-1,i+1}$ of the pre-fractal components, which in the sequel will assume the role of extrema of integration.

[4]Note that, as we deal with masses represented by rectangles, we implicitly assume that the probability measure supported on each pre-fractal component is represented by a (constant) density, which allows for the Riemann definite integrations.

necessarily sum up to a number which is strictly less than 1: it is the area of the rectangle $[x_{t-1,i}, x_{t-1,i+1}] \times [0,1] = \lambda^{t-1} < 1$. This implies that in the formulation above the sum of $\mu_{t,i}$ and $\mu_{t,2^{t-1}+i}$ turns out to be strictly less than the original mass $\mu_{t-1,i}$, which is impossible as that whole mass must be transferred on either $w_1([x_{t-1,i}, x_{t-1,i+1}])$ or $w_2([x_{t-1,i}, x_{t-1,i+1}])$ in the t^{th} pre-fractal and a correction factor of $1/\lambda^{t-1}$ must be introduced in both expressions above, yielding the final formulas[5]

$$\mu_{t,i} = \frac{\int_{x_{t-1,i}}^{x_{t-1,i+1}} p(y)\, \mu_{t-1,i} dy}{\lambda^{t-1}} = \frac{\mu_{t-1,i}}{\lambda^{t-1}} \int_{x_{t-1,i}}^{x_{t-1,i+1}} p(y)\, dy \tag{26}$$

$$\mu_{t,2^{t-1}+i} = \frac{\int_{x_{t-1,i}}^{x_{t-1,i+1}} [1-p(y)]\, \mu_{t-1,i} dy}{\lambda^{t-1}} = \frac{\mu_{t-1,i}}{\lambda^{t-1}} \int_{x_{t-1,i}}^{x_{t-1,i+1}} [1-p(y)]\, dy. \tag{27}$$

Finally, the heights of the newly born rectangles with areas $\mu_{t,i}$ and $\mu_{t,2^{t-1}+i}$ are computed by dividing the numbers above by the length λ^t of the t^{th} pre-fractal components: $m_{t,i} = \mu_{t,i}/\lambda^t$ and $m_{t,2^{t-1}+i} = \mu_{t,2^{t-1}+i}/\lambda^t$. In this second part again two indexes, i and j, are needed, but now the former increases by 2 after each split of the $\mu_{t-1,i}$ mass into the two newly born masses $\mu_{t,i}$ and $\mu_{t,2^{t-1}+i}$ because it denotes the two endpoints of the interval $[x_{t-1,i}, x_{t-1,i+1}]$ on which the single original mass $\mu_{t-1,i}$ is supported, while the latter increases only by 1 because it refers to the single mass $\mu_{t-1,i}$.

The following algorithm summarizes the whole procedure.

Algorithm 1 (Approximates marginal distributions for the IFSP (22))**.**

Step 1 (Initialization): *Set the number n of iterations, the contraction factor $0 < \lambda \leq 1/2$ and the functional form for the state dependent probability $0 < p(y) < 1$ for $y \in [0,1]$. Moreover set the initial endpoints $x_{0,1} = 0$ and $x_{0,2} = 1$ of the $t = 0$ interval (pre-fractal) $A_0 = [0,1]$, and the initial (uniform) mass on it, $\mu_{0,1} = 1$.*

Step 2 (Generate pre-fractals and 'rectangle masses'): *For t from 1 to n do:*

1. *set $i = 1$ and $j = 1$,*
2. *while $i \leq 2^t$ and $j \leq 2^{t+1}$ do:*
   (a) *(define endpoints of t^{th} pre-fractal components) set $x_{t,j} = x_{t-1,i}$, $x_{t,j+1} = x_{t-1,i} + \lambda^t$, $x_{t,j+2} = x_{t-1,i+1} - \lambda^t$, $x_{t,j+3} = x_{t-1,i+1}$,*
   (b) *(update indexes i and j and move to the next component on the $(t-1)^{th}$ pre-fractal) set $i = i + 2$, $j = j + 4$;*
3. *reset $i = 1$ and $j = 1$,*
4. *while $i \leq 2^{t-1}$ and $j \leq 2^t$ do:*
   (a) *(split the mass $\mu_{t-1,i}$ on each component of the $(t-1)^{th}$ pre-fractal into masses on $w_1([x_{t-1,i}, x_{t-1,i+1}])$ and $w_2([x_{t-1,i}, x_{t-1,i+1}])$ of the t^{th} pre-fractal) set $\mu_{t,i} = (\mu_{t-1,i}/\lambda^{t-1}) \int_{x_{t-1,j}}^{x_{t-1,j+1}} p(y)\, dy$, $\mu_{t,2^{t-1}+i} = (\mu_{t-1,i}/\lambda^{t-1}) \int_{x_{t-1,j}}^{x_{t-1,j+1}} [1-p(y)]\, dy$, $m_{t,i} = \mu_{t,i}/\lambda^t$, $m_{t,2^{t-1}+i} = \mu_{t,2^{t-1}+i}/\lambda^t$,*

[5]Note that equations (26) and (27) reduce to the standard probability assignment on the t^{th} pre-fractal when probabilities are constant, $p_1 \equiv p$ and $p_2 \equiv 1-p$, which is given by $\mu_{t,i} = p\mu_{t-1,i}$ and $\mu_{t,2^{t-1}+i} = (1-p)\, \mu_{t-1,i}$.

(b) (update indexes i and j and move to the next mass on the $(t-1)^{th}$ pre-fractal) set $i = i + 1$, $j = j + 2$.

Step 3 (Produce and plot the approximation of the n^{th} marginal distribution):

1. *Set $i = 1$, $j = 1$ and set (null vector of rectangles) $X = [\quad]$,*
2. *while $i \leq 2^{n-1}$ and $j \leq 2^n$ do:*
   (a) (generate a vector of rectangles each representing the mass on each component of the n^{th} pre-fractal) add the rectangle $[x_{n,i}, x_{n,i+1}] \times [0, m_{n,j}]$ to the vector X,
   (b) (update indexes i and j and move to the next rectangle on the n^{th} pre-fractal) set $i = i + 2$, $j = j + 1$;
3. *plot the vector X containing the rectangles just generated.*

It should be noted that the well known algorithm based on the "Chaos game" (see, *e.g.*, [3] or, more recently, [14]) may be applied in this case as well. Its advantage with respect to Algorithm 1 is less computational effort required, as it yields directly an approximation of the invariant measure in the form of an Histogram obtained just by iterating the maps w_1 and w_2 in the IFSSDP (22) a sufficiently large number of times according to probabilities $p(x)$ and $1 - p(x)$ starting from any point $x_0 \in [0, 1]$, and counting how many times the trajectory enters each sub-interval in a partition of $[0, 1]$ of M sub-intervals, each of of length $1/M$, for M sufficiently large. Unlike this approach, our Algorithm 1 allows for keeping track of the evolution of the initial uniform probability on $[0, 1]$ at each iteration t, so that the effect of the state-dependent probabilities $p(x)$ and $1 - p(x)$ on the maps w_1 and w_2 is being emphasized by how the masses (rectangles) on each t^{th} pre-fractal are transformed on new masses generated on the newly born $(t+1)^{th}$ pre-fractals after the next iteration. Such evolution can be appreciated in the next Figures 1 and 2, where the whole transition from the uniform measure on $[0, 1]$ to the approximation of the invariant measure in Figures 1(i) and 2(i) is plotted through all first nine iterations of Algorithm 1. Admittedly, our approach is more computationally intensive than the "Chaos game" procedure; however, we believe that the purposeful contribution of Algorithm 1 is a dynamic one, by allowing to study how the state-dependent probabilities affect the geometric transformation of the marginal measures after each single iteration of the IFSSDP (22). Moreover, as nine iterations are enough to get a good approximation of the invariant measure, all plots in the next Section are obtained in few seconds.

5 Applying Algorithm 1 to our Stochastic Growth Model

To be precise, Algorithm 1 uses the probabilities of the 'linearization' x of the reduced variable $\chi = h/k$ according to the log-linear transformation (19), that is, those labelled as $\tilde{p}(x)$ in (21), rather than the original probability function $p(\chi)$ associated to the reduced variable $\chi = h/k$. In the following examples we shall consider *monotone state-dependent probabilities* for the linear IFSSDP (22), that, consistent with the notation adopted in Algorithm 1, will be denoted by $\tilde{p}(y)$ rather than by $\tilde{p}(x)$, as the $x_{t,i}$s denote endpoints of the t^{th} pre-fractal components. Under the assumptions that $\inf\{\tilde{p}(y) : 0 \leq y \leq 1\} > 0$ and $\tilde{p}$ is Hölder continuous the results in Section 2.2 guarantee that the IFSSDP (22) defined on the space $X = [0, 1]$ converges to a unique invariant measure $\bar{\mu}_\lambda$ supported on the attractor $\bar{A}$ defined in Corollary 1. We shall further assume that $\lambda < 1/2$, so that, according to Proposition 1, the attractor $\bar{A}$ is a Cantor-like set and the invariant measure $\bar{\mu}_\lambda$ is singular with respect to the Lebesgue measure. Using the probability transformation

in (21) we can easily recover the state-dependent probability governing the original nonlinear reduced variable $\chi = h/k$ as:

$$p(\chi) = \tilde{p}(y) = \tilde{p}\left(-\frac{1-\lambda}{\ln r}\ln\chi + 1 + \frac{\ln\Lambda}{\ln r}\right), \tag{28}$$

where in the second equality we used (19). Note that probability $p(\chi)$ is defined on the same space as that of the nonlinear system (16), that is, the interval $\left[(r\Lambda)^{\frac{1}{1-\lambda}}, \Lambda^{\frac{1}{1-\lambda}}\right]$, whose endpoints are the two nontrivial fixed points of the maps $w_1(\chi) = r\Lambda\chi^\lambda$ and $w_2(\chi) = \Lambda\chi^\lambda$ respectively. Moreover, $\inf\left\{p(\chi) : (r\Lambda)^{\frac{1}{1-\lambda}} \leq \chi \leq \Lambda^{\frac{1}{1-\lambda}}\right\} > 0$, $\sup\left\{p(\chi) : (r\Lambda)^{\frac{1}{1-\lambda}} \leq \chi \leq \Lambda^{\frac{1}{1-\lambda}}\right\} < 1$ and p is Hölder continuous because the argument y of $\tilde{p}$ in the RHS of (28) is a continuous, strictly increasing function of χ (as $-\ln r > 0$), being 0 when $\chi = (r\Lambda)^{\frac{1}{1-\lambda}}$ and 1 when $\chi = \Lambda^{\frac{1}{1-\lambda}}$. Therefore, the random dynamical system $\chi_{t+1} = z_t\Lambda\chi_t^\lambda$ defined in (16) is an homeomorphism conjugate to the linear system (20)—or, equivalently (22)—and thus itself converges to a unique singular invariant measure supported on a distorted Cantor-like set contained in the interval $\left[(r\Lambda)^{\frac{1}{1-\lambda}}, \Lambda^{\frac{1}{1-\lambda}}\right]$.

In order to shed some light on how the invariant measure may look like, and on how it is affected by different state-dependent probabilities $\tilde{p}(y)$, in the sequel we run Algorithm 1 for some examples of $\tilde{p}(y)$. We consider the following values for some of the parameters:

$$\theta = 12, \qquad \alpha = 0.67, \qquad \beta = 0.18, \qquad r = u = 0.5. \tag{29}$$

All values above envisage a sufficiently large θ [see condition (17)] and allow for a range $[\bar{s}_1, \bar{s}_r]$ for the saving rate s that permits to consider both the first and second scenarios at the end of Subsection 3.2, that is, wandering randomly between one dynamic pushing toward sustained growth and one leading to asymptotic extinction, and randomly jumping between two trajectories both converging to balanced growth paths characterized by sustained growth but at different growth rates. Specifically, according to (18) the values of the bounds $\bar{s}_1$ and $\bar{s}_r$ become:

$$\bar{s}_1 = \frac{1}{\theta u^\alpha (1-u)^{1-\alpha}} = 0.1333 \qquad \text{and} \qquad \bar{s}_r = \frac{1}{\theta u^\alpha \left[r^{\frac{1}{\beta}}(1-u)\right]^{1-\alpha}} = 0.4751,$$

so that, for example, when $s = 0.3$ the system is randomly being stretched between dynamics asymptotically converging either to null or to sustained balanced growth, while if $s = 0.6$ the system grows in time, although at (positive) growth rates that change as time elapses.

The values for α and β imply that $\lambda = \alpha - \beta = 0.49$, just below $1/2$, which means that the linear IFSSDP (22) converges to a unique singular invariant measure supported over a Cantor set that almost fills the whole interval $[0, 1]$. Such an assumption is justified by our interest in thoroughly investigating the role of state-dependent probabilities: having pre-fractals that almost cover $[0, 1]$ in Algorithm 1 means that the state-dependent probabilities affect the system on most points in their domain; in other words, their shape gives an important contribution in determining the invariant measure $\bar{\mu}_\lambda$. For such parameters' values the trapping region of the corresponding nonlinear system (16) becomes the interval $[\chi_r^*, \chi^*] = \left[(r\Lambda)^{\frac{1}{1-\lambda}}, \Lambda^{\frac{1}{1-\lambda}}\right] = [0.0067, 0.0262]$.

In the following examples we shall just assume that $\lambda = 0.49$, so that the economy described by the parameters' values in (29) belongs to the family of economies for which we aim at approximating their invariant measure. Note, however, that, as Algorithm 1 requires only the parameter $\lambda = \alpha - \beta$ to work, our simulations turn out to be independent of all parameters' values in (29)

except of the difference $\alpha - \beta$, moreover, they are also independent of the saving rate; specifically, any value of saving rate $0 < s < 1$ can be associated to our simulations, including values $s < \bar{s}_1 = 0.1333$ envisaging dynamics all leading to extinction, although at different rates through time.

Figure 1 illustrates the working of Algorithm 1 by showing its first $n = 9$ iterations performed by Maple for the state-dependent probability defined by $\tilde{p}(y) = 0.98y + 0.01$, satisfying $\tilde{p}(y) > 0$ and $1 - \tilde{p}(y) > 0$ for all $y \in [0, 1]$, which is increasing and affine. Such a probability represents a "smoothing" process that tends to concentrate the weight of the random variable x_t of the IFSSDP (20) on the fractal components that lie in the middle of the interval $[0, 1]$. Specifically, it puts a smaller probability on the lower map w_1—so that the probability of the higher map w_2 is larger—when x_t is small, thus favoring higher values for x_{t+1} when x_t approaches the left endpoint of $[0, 1]$, while it puts a higher probability on the lower map w_1—so that the probability of the higher map w_2 is lower—when x_t is closer to 1, thus favoring lower values for x_{t+1} when x_t approaches the right endpoint of $[0, 1]$. As confirmed by the plots in the figure, such system concentrates most of the mass in the middle of the interval $[0, 1]$, although such mass is very irregularly distributed because the invariant measure is singular. Note that already after the 5^{th} iteration in Figure 1(e) the approximation of the marginal distribution μ_5 assumes qualitative traits that are maintained in the subsequent iterations; this implies that our algorithm exhibits the main characteristic traits that must feature in the limit invariant measure $\bar{\mu}_\lambda$, at least qualitatively.

Figure 2 shows the first $n = 9$ iterations of Algorithm 1 performed by Maple for the state-dependent probability defined by $\tilde{p}(y) = 0.99 - 0.98y$, satisfying $\tilde{p}(y) > 0$ and $1 - \tilde{p}(y) > 0$ for all $y \in [0, 1]$, which is again affine but now is decreasing. Contrary to the previous example, such probability represents a conservative process that polarizes the system by concentrating the weight of the random variable x_t close to the endpoints 0 and 1. Specifically, it puts a larger probability on the lower map w—so that the probability of the higher map w_2 is smaller—when x_t is small, while it puts a smaller probability on the lower map w_1—so that the probability of the higher map w_2 is larger—when x_t is closer to 1. As confirmed by the plots in the figure, such a system increases inequality through time, concentrating most of the mass—but not all, as $\tilde{p}(y) > 0$ and $1 - \tilde{p}(y) > 0$—on the endpoints of the interval $[0, 1]$.

Figure 3 reports only the 9^{th} iteration of Algorithm 1 implemented by Maple for four nonlinear variants of the previous two state-dependent probabilities. Specifically, in Figure 3(a) we use $\tilde{p}(y) = 0.98y^4 + 0.01$, which is increasing and convex, concentrating most of the weight on the higher map w_2, thus favoring higher values for x_{t+1}, when x_t take values up to around 0.75, while concentrating most of the weight on the lower map w_1, thus favoring lower values for x_{t+1}, when x_t take values closer to 1. The figure shows a measure that somewhat resembles the traits of the measure in Figure 1(i), only concentrating more mass on the right part of the interval $[0, 1]$; that is, consistent with the increasing monotonicity of $\tilde{p}$, this system tends to put most of the mass on points which are interior to $[0, 1]$, the convexity of $\tilde{p}$ implying a larger mass to the right. A similar picture is provided by Figure 3(b), where $\tilde{p}(y) = 0.99 - 0.98(y - 1)^4$ has been used, which is increasing and concave, concentrating most of the weight on the lower map w_1, thus favoring lower values for x_{t+1}, when x_t take values larger than 0.25, while concentrating most of the weight on the higher map w_2, thus favoring lower values for x_{t+1}, when x_t take values closer to 0. Again the figure shows a measure that somewhat resembles the traits of the measure in Figure 1(i), only concentrating more mass on the left part of the interval $[0, 1]$; that is, consistent with the increasing monotonicity of $\tilde{p}$, this system tends to put most of the mass on points which are interior to $[0, 1]$, the concavity of $\tilde{p}$ implying a larger mass to the left.

If a decreasing, convex state-dependent probability is used instead, like $\tilde{p}(y) = 0.98(y - 1)^4 +$

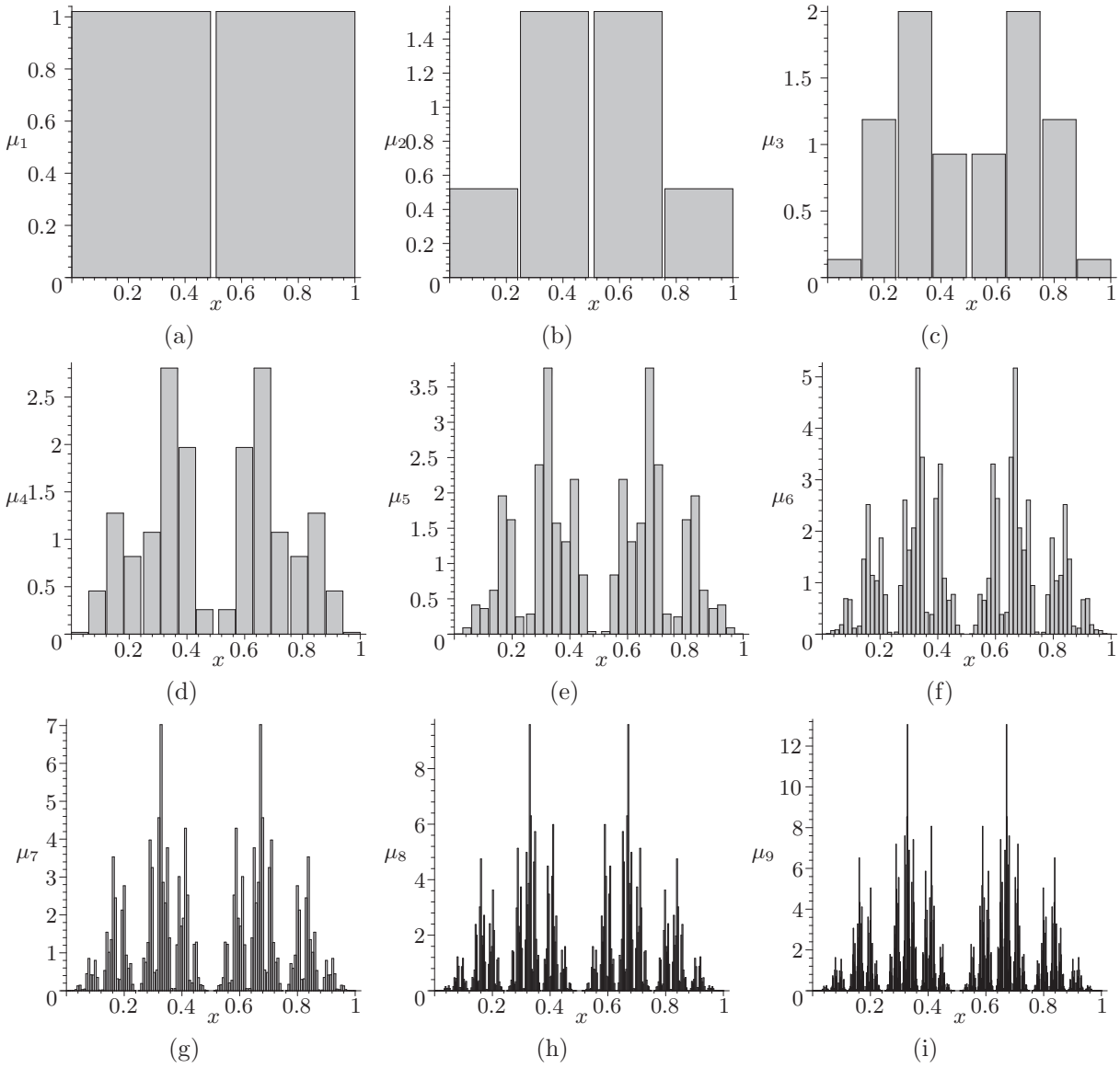

FIGURE 1: First 9 iterations of Algorithm 1 for $\lambda = 0.49$ and $\tilde{p}(y) = 0.98y + 0.01$.

0.01 that concentrates most of the weight on the higher map w_2, thus favoring higher values for x_{t+1}, when x_t take values larger than 0.25, while concentrating most of the weight on the lower map w_1, thus favoring lower values for x_{t+1}, when x_t take values closer to 0, the measure ends up concentrating most of the mass close to the right endpoint 1, as it is apparent from Figure 3(c); it somewhat resembles the traits of the measure in Figure 2(i), only concentrating mass almost exclusively around 1; that is, consistent with the decreasing monotonicity of $\tilde{p}$, this system tends to put most of the mass close to the endpoints 0 and 1 of $[0, 1]$, the convexity of $\tilde{p}$ implying a larger mass to the right. Conversely, if a decreasing, concave state-dependent probability is used instead, like $\tilde{p}(y) = 0.99 - 0.98y^4$ that concentrates most of the weight on the lower map w_1, thus favoring higher values for x_{t+1}, when x_t take values up to around 0.75, while concentrating most of the weight on the higher map w_2, thus favoring higher values for x_{t+1}, when x_t take values closer to 1, the measure ends up concentrating most of the mass close to the left endpoint 1, as shown in Figure 3(d); again the traits of the measure in Figure 2(i) are maintained, only concentrating

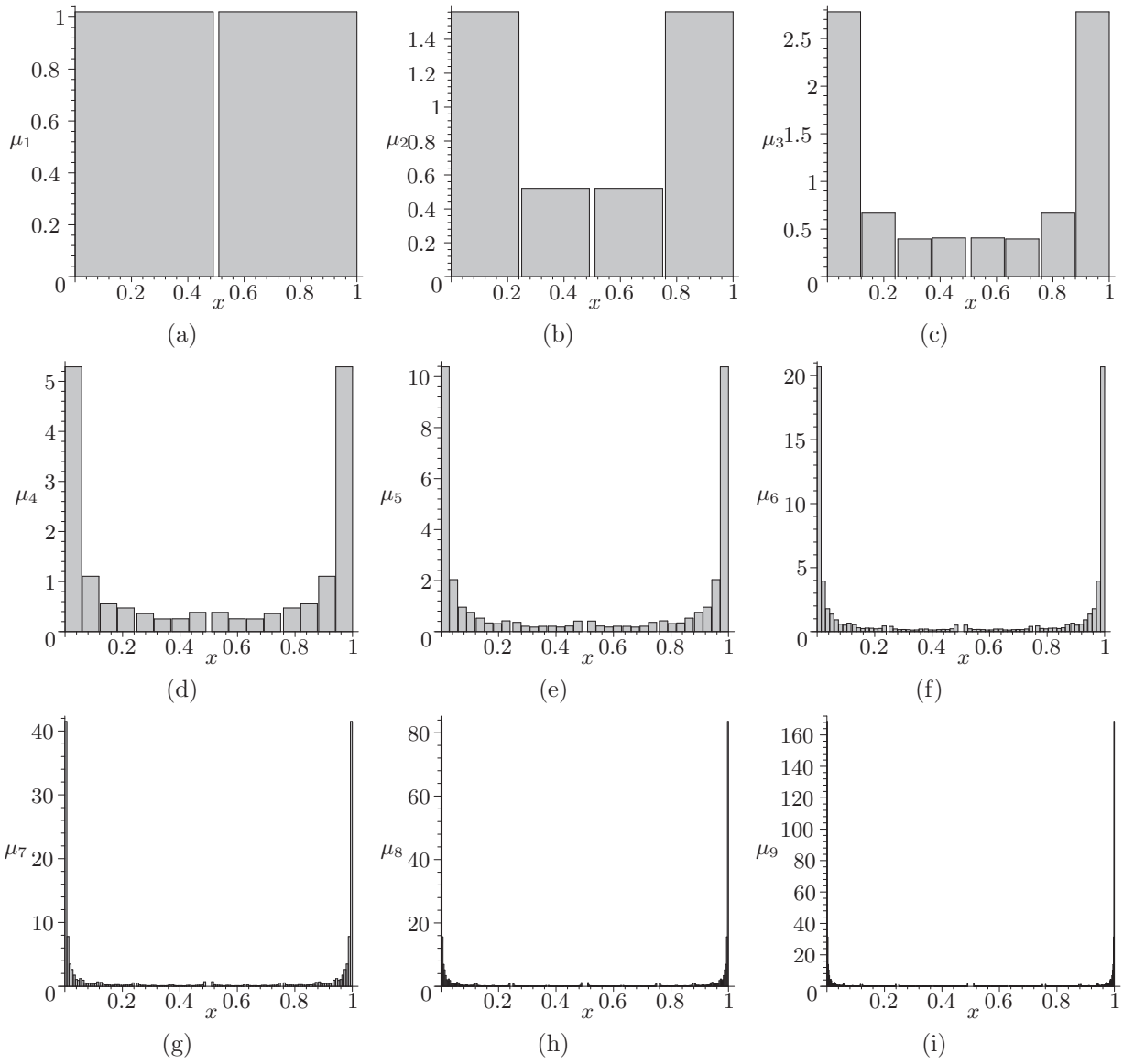

FIGURE 2: First 9 iterations of Algorithm 1 for $\lambda = 0.49$ and $\tilde{p}(y) = 0.99 - 0.98y$.

mass almost exclusively around 0; that is, consistent with the decreasing monotonicity of $\tilde{p}$, this system tends to put most of the mass close to the endpoints 0 and 1 of $[0, 1]$, the concavity of $\tilde{p}$ implying a larger mass to the left.

Finally, in Figure 4 we tentatively attempt two comparisons between constant probabilities at $\tilde{p}$ and $1-\tilde{p}$ values and the simplest state-dependent counterparts defined as piecewise constant/affine functions: Figures 4(a) and 4(b) report the 9^{th} iteration of Algorithm 1 implemented by Maple for constant probabilities $\tilde{p} \equiv 0.333$ and $\tilde{p} \equiv 0.667$ respectively, while Figures 4(c) and 4(d) report

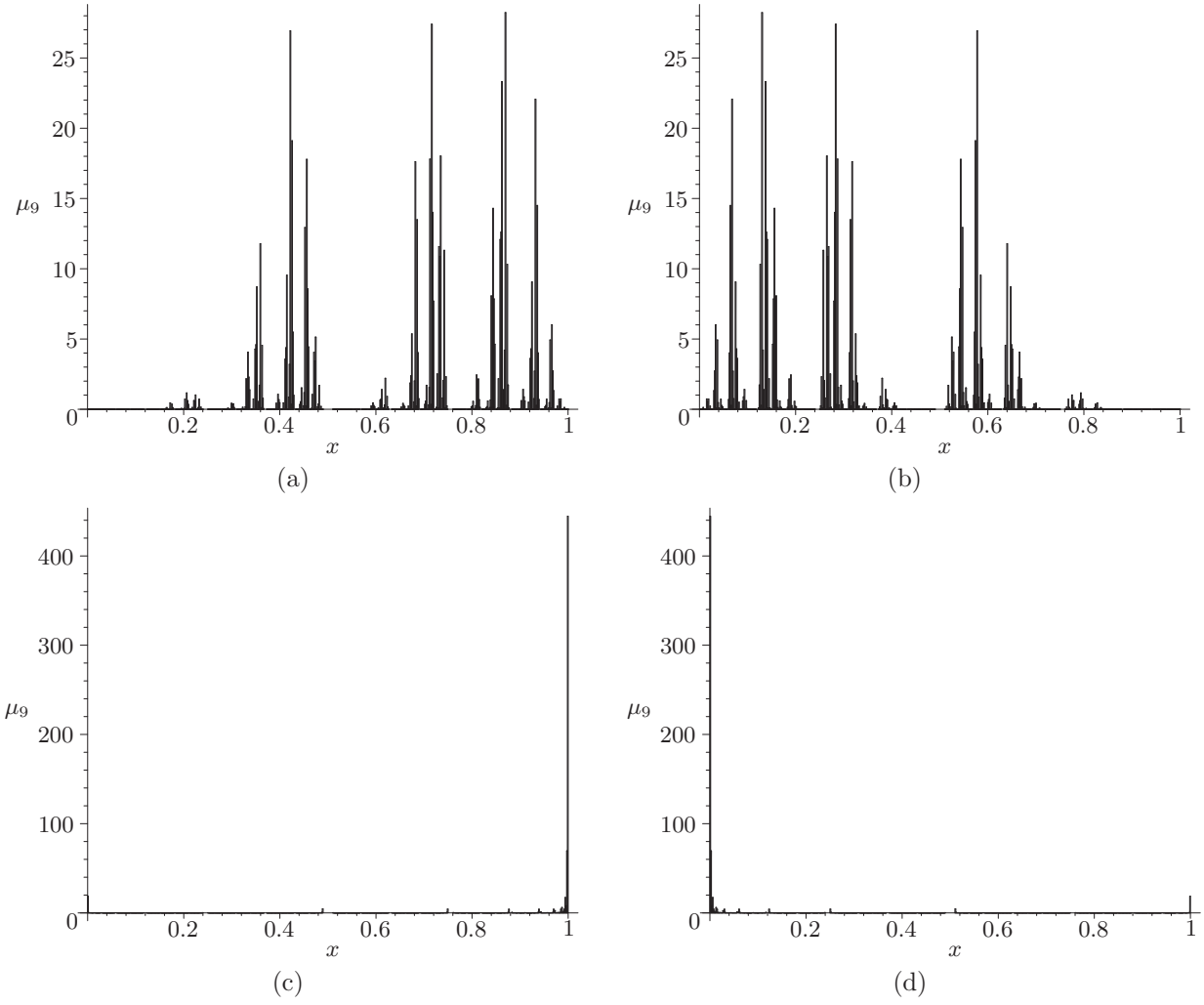

FIGURE 3: 9^{th} iteration of Algorithm 1 for $\lambda = 0.49$ and a) $\tilde{p}(y) = 0.98y^4 + 0.01$, b) $\tilde{p}(y) = 0.99 - 0.98(y-1)^4$, c) $\tilde{p}(y) = 0.98(y-1)^4 + 0.01$, d) $\tilde{p}(y) = 0.99 - 0.98y^4 + 0.01$.

the 9^{th} iteration of Algorithm 1 implemented by Maple for the piecewise probabilities defined as

$$\tilde{p}(y) = \begin{cases} 0.333 & \text{for } 0 \le y < 0.49 \\ 16.7y - 7.85 & \text{for } 0.49 \le y < 0.51 \\ 0.667 & \text{for } 0.51 \le y \le 1 \end{cases} \quad \text{and} \tag{30}$$

$$\tilde{p}(y) = \begin{cases} 0.667 & \text{for } 0 \le y < 0.49 \\ 8.85 - 16.7y & \text{for } 0.49 \le y < 0.51 \\ 0.333 & \text{for } 0.51 \le y \le 1 \end{cases} \tag{31}$$

respectively. The latter probabilities in (30) and (31) are continuous and constant on the two components of the first pre-fractal, *i.e.* on the intervals $[0, 0.49]$ and $[0.51, 1]$, while they are affine and steeply sloped—the former increasing and the latter decreasing—on the open interval $(0.49, 0.51)$, which turns out to be irrelevant for the iterations of Algorithm 1 as it contains only points that will never appear in the chaos game. They are both Hölder continuous, so that existence and uniqueness of the invariant measure $\bar{\mu}_\lambda$ is assured. Figures 4(a) and 4(b) show the well-known features of two singular measures that concentrate more mass on the right part and in the left part

of $[0,1]$ respectively. Conversely, Figures 4(c) and 4(d) again exhibit a feature already encountered in the previous plots: depending on whether $\tilde{p}(y)$ is increasing or decreasing (weakly in this case) the mass is being concentrated toward the inner part of $[0,1]$ in the former case while it is being concentrated toward the endpoints of $[0,1]$ in the latter case; that is, increasing probabilities have a "smoothing" effect cutting out the edges while decreasing probabilities increase the polarization of the system. In this peculiar scenario both also happen to transform the unbalanced measures in Figures 4(a) and 4(b), which are skewed to the right and to the left respectively, into perfectly symmetric measures.

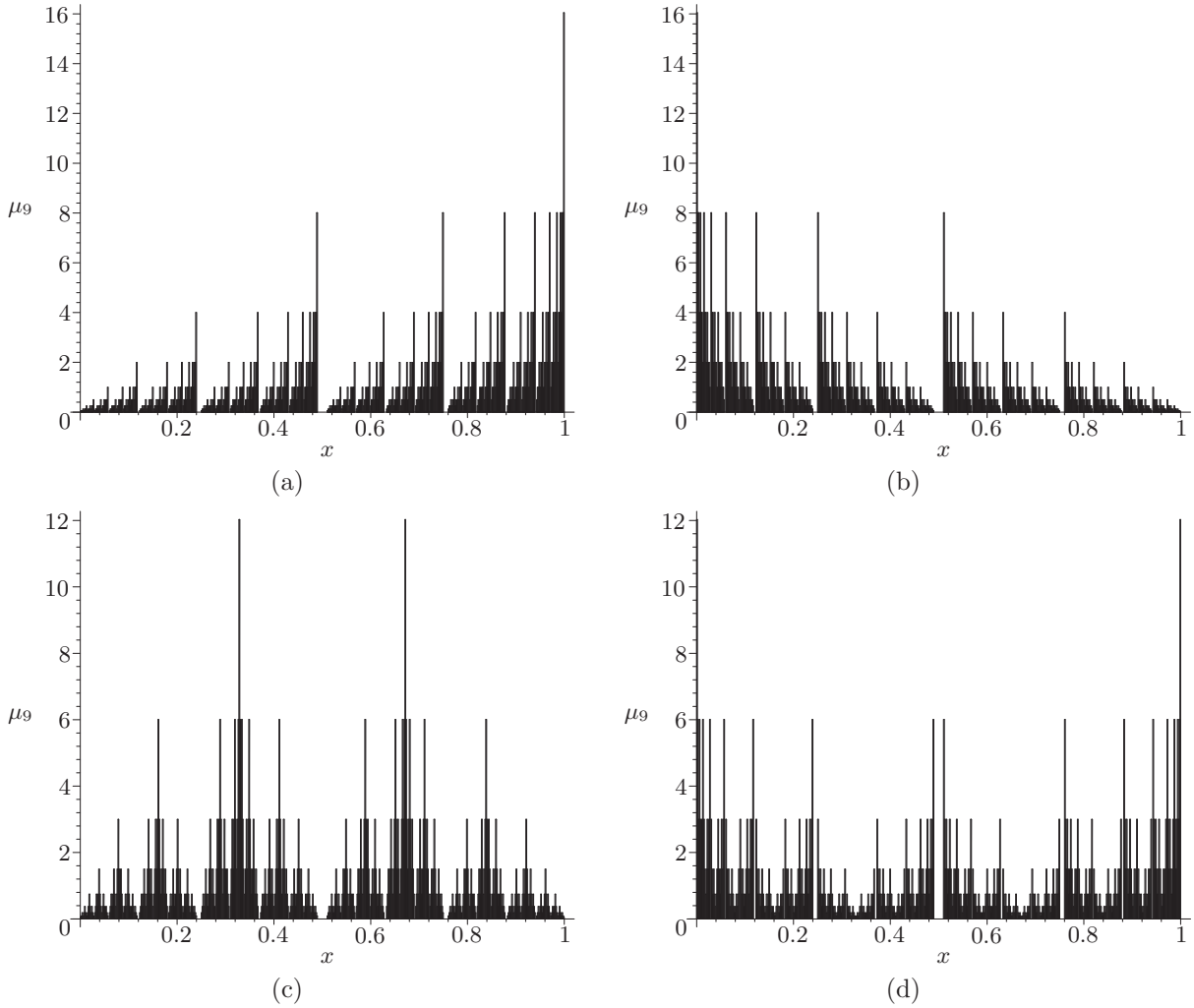

FIGURE 4: 9^{th} iteration of Algorithm 1 for $\lambda = 0.49$ and a) $\tilde{p} \equiv 0.333$, b) $\tilde{p} \equiv 0.667$, c) $\tilde{p}$ defined as a piecewise function in (30), d) $\tilde{p}$ defined as a piecewise function in (31).

The above analysis allows us to derives some interesting conclusions. First, allowing probabilities to be state dependent increases the number of possible outcomes. Second, assuming simplistically that probabilities are constant does not necessarily provide us with an even rough approximation of the outcome under state dependent probabilities. These results suggest that formally taking into account the state-dependency of probabilities is important not only to develop a more realistic framework to characterize economic outcomes, but also to understand which outcomes may effectively occur.

6 Conclusion

Several studies discuss how the degree of vulnerability to shocks changes from one economy to the next according to their specific individual characteristics, suggesting the existence of path-dependency in the process of economic development. In order to analyze path-dependency in macroeconomic dynamics, we analyze a two-sector discrete time stochastic growth model driven by physical and health capital accumulation in which shock probabilities are state-dependent. State-dependent probabilities represent an interesting generalization of classical constant probabilities both from a mathematical and an economic point of view, since they allow to enrich the set of possible model's outcomes and to describe more realistically economic dynamics. We show that our model's dynamics can be converted into an iterated function system with state-dependent probabilities, which converges to an invariant self-similar measure supported on a (possibly fractal) compact attractor. We develop a numerical method to approximate the invariant measure of our iterated function system with state-dependent probabilities to illustrate the implications of such state-dependent probabilities on the steady state of our stochastic growth model, and we show that the model's long run outcome under state-dependent and constant probabilities may be very different, suggesting that neglecting the state-dependence of probabilities may lead to misleading conclusions about long run macroeconomic outcomes.

To the best of our knowledge this is the first paper introducing state-dependent probabilities in economics. To exemplify the variety of possible outcomes that state-dependent probabilities can lead to, we focus on a very stylized purely dynamic model, completely abstracting from agents' optimization. Introducing agents' optimization adds a further layer of complexity to the analysis since rational agents, by realizing that their decisions affect state variables and thus probabilities, account for the eventual time evolution of probabilities in the determination of their best choices. Analyzing the extent to which agents' optimization in a framework with state dependent probabilities differs from a traditional setting with constant probabilities is left for future research.

References

[1] Aghion P, Howitt P, Murtin F. The relationship between health and growth: when Lucas meets Nelson–Phelps. Review of Economics and Institutions 2011;2: article 1.

[2] Barnsley MF. Fractals everywhere. New York: Academic Press; 1989.

[3] Barnsley MF, Demko S, Elton J, Geronimo J. Invariant measures for Markov processes arising from iterated function systems with place-dependent probabilities. Ann Inst H Poincaré Prob Stat 1988;24:367–394. Erratum 1990;25:589–590.

[4] Barro RJ. Health and economic growth, Annals of Economics and Finance 2013;14:329–366.

[5] Barro RJ, Sala-i-Martin X. Economic growth. 2nd Edition. Cambridge: MIT Press; 2004.

[6] Boucekkine R, Ruiz–Tamarit JR. Imbalance effects in the Lucas Model: an analytical exploration. B.E. Journal in Macroeconomics (Topics in Macroeconomics) 2004; article 15.

[7] Brock WA, Mirman LJ. Optimal Economic Growth and Uncertainty: the Discounted Case. Journal of Economic Theory 1972;4:479–513.

[8] Hutchinson J. Fractals and self-similarity. Indiana Univ J Math 1981;30:713–747.

[9] Elton J. An ergodic theorem for iterated maps. J Erg Theory Dyn Sys 1987;7**:**481–488.

[10] Krugman P. Increasing returns and economic geography. Journal of Political Economy 1991;99:483–499.

[11] Kunze H, La Torre D, Mendivil F, Vrscay ER. Fractal-based methods in analysis. New York: Springer; 2012.

[12] La Torre D, Marsiglio S, Privileggi F. Fractals and self-similarity in economics: the case of a two-sector growth model. Image Analysis & Stereology 2011;30:143–151.

[13] La Torre D, Marsiglio S, Mendivil F, Privileggi F. Self-similar measures in multi-sector endogenous growth models. Chaos, Solitons and Fractals 2015;79:40–56.

[14] La Torre D, Maki E, Mendivil F, Vrscay ER. Iterated function systems with place-dependent probabilities and the inverse problem of measure approximation using moments. Fractals 2018a;26:1850076.

[15] La Torre D, Marsiglio S, Privileggi F. Fractal attractors in economic growth models with random pollution externalities. Chaos 2018b;28:055916.

[16] La Torre D, Marsiglio S, Mendivil F, Privileggi F. Fractal attractors and singular invariant measures in two-sector growth models with random factor shares. Communications in Nonlinear Science and Numerical Simulation 2018c;58:185–201.

[17] Marsiglio S. Stochastic shocks in a two-sector Solow model. International Journal of Mathematical Modelling and Numerical Optimisation 2012;3:313–318.

[18] Martin R, Sunley P. Path dependence and regional economic evolution. Journal of Economic Geography 2006;6:395—437.

[19] Mitra T, Montrucchio L, Privileggi F. The nature of the steady state in models of optimal growth under uncertainty. Econ Theor 2003;23:39–71.

[20] Mitra T, Privileggi F. Cantor type invariant distributions in the theory of optimal growth under uncertainty. J Difference Equ Appl 2004;10:489–500.

[21] Mitra T, Privileggi F. Cantor type attractors in stochastic growth models. Chaos, Solitons and Fractals 2006;29:626–637.

[22] Mitra T, Privileggi F. On Lipschitz continuity of the iterated function system in a stochastic optimal growth model. J Math Econ 2009;45:185–198.

[23] Montrucchio L, Privileggi F. Fractal steady states in stochastic optimal control models. Ann Oper Res 1999;88:183–197.

[24] Mullingan CB, Sala-i-Martin X. Transitional dynamics in two-sector models of endogenous growth. Quarterly Journal of Economics 1993;108:739–773.

[25] North DC. Economic performance through time. American Economic Review 1994;84:359–368.

[26] Olson LJ, Roy S. Theory of stochastic optimal economic growth. In: Dana RA, Le Van C, Mitra T, Nishimura K, editors. Handbook on optimal growth 1: discrete time. New York: Springer; 2005. p. 297–336.

[27] Privileggi F, Marsiglio S. Environmental shocks and sustainability in a basic economy-environment model. Int J Applied Nonlinear Science 2013;1:67–75.

[28] Solow R. A contribution to the theory of economic growth. Q J Econ 1956;70:65–94.

[29] Stenflo Ö. Uniqueness of invariant measures for place-dependent random iteration of functions. Fractals in Multimedia. In: The IMA Volumes in Mathematics and its Application book series 2002;132:13–32.

[30] Stenflo Ö. A survey of average contractive iterated function systems. J Difference Eq Appl 2012;18(8):1355–1380.

[31] Tai, M.Y., Chao, C.C., Hu, W.W. Pollution, health and economic growth. North American Journal of Economics and Finance 2015;32:155–161.

[32] Varangis P, Varma S, dePlaa A, Nehru V. Exogenous shocks in low income countries: economic policy issues and the role of the international community. The World Bank; 2004.

[33] van Zon A, Muysken J. Health and endogenous growth. Journal of Health Economics 2001;20:169–185.